HHS Public Access

Author manuscript

Oncogene. Author manuscript; available in PMC 2024 October 03.

Published in final edited form as:

Oncogene. 2024 April ; 43(15): 1087–1097. doi:10.1038/s41388-024-02966-w.

The BAP1 nuclear deubiquitinase is involved in the nonhomologous end-joining pathway of double-strand DNA repair through interaction with DNA-PK

Hiroki Sato[1,*], **Tatsuo Ito**[1,2,*], **Takuo Hayashi**[1], **Shigehisa Kitano**[3], **Hediye Erdjument-Bromage**[4], **Matthew J. Bott**[5], **Shinichi Toyooka**[6], **Marjorie Zauderer**[7], **Marc Ladanyi**[1,8]

[1]Department of Pathology and Laboratory Medicine, Memorial Sloan Kettering Cancer Center, New York, NY, USA

[2]Department of Hygiene, Kawasaki Medical University, Okayama, Japan

[3]Immunology Program, Memorial Sloan Kettering Cancer Center, New York, NY, USA

[4]Kimmel Center for Biology and Medicine at Skirball Institute, Department of Biochemistry and Molecular Pharmacology, New York University School of Medicine, New York, New York 10016, United States.

[5]Thoracic Service, Department of Surgery, Memorial Sloan Kettering Cancer Center, New York, NY

[6]Department of Thoracic, Breast and Endocrinological Surgery, Okayama University Graduate School of Medicine, Dentistry and Pharmaceutical Sciences, Okayama, Japan

[7]Thoracic Oncology Service, Department of Medicine, Memorial Sloan Kettering Cancer Center, New York, NY

[8]Human Oncology & Pathogenesis Program, Memorial Sloan Kettering Cancer Center, New York, New York, USA

Abstract

BRCA1-associated protein 1 (BAP1) has emerged as a major tumor suppressor gene in diverse cancer types, notably in malignant pleural mesothelioma (DPM), and has also been identified as a germline cancer predisposition gene for DPM and other select cancers. However, its role in the response to DNA damage has remained unclear. Here, we show that BAP1 inactivation is associated with increased DNA damage both in Met-5A human mesothelial cells and human

[#]**Address correspondence to:** Marc Ladanyi, MD, Dept. of Pathology and Laboratory Medicine, Room S-801, MSKCC, 1275 York Avenue, New York, NY10065, ladanyim@mskcc.org.

[*]These authors contributed equally to this study.

Contributions

TI and ML conceptualized the project. TI designed the experiments. TI and TH performed experiments. HEB helped with proteomics studies. MJB provided data. SK and ST provided advice and guidance. MGZ provided clinical context. HS and ML finalized the manuscript. ML provided overall supervision of the project.

Conflict of interest disclosure statements:

The authors declare no potential conflicts of interest.

Ethics declarations / Competing interests

The authors declare no competing interests.

DPM cell lines. Through proteomic analyses, we identified PRKDC as an interaction partner of BAP1 protein complexes in DPM cells and 293T human embryonic kidney cells. PRKDC encodes the catalytic subunit of DNA protein kinase (DNA-PKcs) which functions in the nonhomologous end-joining (NHEJ) pathway of DNA repair. Double-stranded DNA damage resulted in prominent nuclear expression of BAP1 in DPM cells and phosphorylation of BAP1 at serine 395. A plasmid-based NHEJ assay confirmed a significant effect of BAP1 knockdown on cellular NHEJ activity. Combination treatment with X-ray irradiation and gemcitabine (as a radiosensitizer) strongly suppressed the growth of BAP1-deficient cells. Our results suggest reciprocal positive interactions between BAP1 and DNA-PKcs, based on phosphorylation of BAP1 by the latter and deubiquitination of DNA-PKcs by BAP1. Thus, functional interaction of BAP1 with DNA-PKcs supports a role for BAP1 in NHEJ DNA repair and may provide the basis for new therapeutic strategies and new insights into its role as a tumor suppressor.

Keywords

Malignant pleural mesothelioma; BAP1; nonhomologous end-joining; DNA-PKcs

Introduction

In the past decade, there has been a considerable effort to better characterize the molecular pathogenesis of malignant diffuse pleural mesothelioma (DPM), a highly lethal cancer arising from the mesothelial cells lining the chest cavity [14]. Genomic profiling studies first identified BAP1 as a frequently inactivated gene in DPM, with deletion, mutation, or both in up to 42% of cases [5]. More recent genomic data suggest that the prevalence of BAP1 inactivation in DPM may be close to 60% [20]. Inactivating somatic mutations of *BAP1* are also common in uveal melanomas, primarily in the metastasizing subset where the *BAP1* mutation rate approaches 80% [18]. BRCA1-associated protein 1 (BAP1) is a 729-amino acid nuclear ubiquitin hydrolase that has been implicated in cell proliferation, chromatin regulation, and DNA repair response [23]. As further evidence of its tumor suppressor function, germline *BAP1* mutations are found in families predisposed to DPM and uveal melanomas [44, 48]. The tumor spectrum of the Germline BAP1 syndrome now also includes several other cancers in which it has also been found to be commonly inactivated somatically [9]. BAP1 has also been confirmed to behave as a classic tumor suppressor in mice carrying heterozygous germline BAP1 mutations [24].

One of the functions first postulated for BAP1 was in the DNA repair response to double-strand breaks (DSBs) [23]. These are repaired via two major pathways: homologous recombination (HR) and nonhomologous end-joining (NHEJ) [19]. NHEJ involves binding of the Ku70/Ku80 (Ku) protein to DNA termini which ensures alignment of the ends of the DNA strands and recruitment of the catalytic subunit of DNA-dependent protein kinase (DNA-PKcs) [8, 46, 49]. DNA-PKcs then stimulates processing of the aligned DNA strands [32, 49]. To date, the best described phosphorylation target of DNA-PKcs is DNA-PKcs itself; several autophosphorylation sites in DNA-PKcs have been identified and it is phosphorylated *in vivo* upon DNA damage. Importantly, cells defective in DNA-PKcs have increased sensitivity to radiation [3, 11, 32, 46, 49]. While some previous studies provided

experimental evidence that BAP1 is involved in HR [22, 27, 52], pre-clinical studies [39, 50] and clinical trials based on the notion that BAP1 loss might make DPM more sensitive to PARP inhibition have been uniformly disappointing[15, 16, 38]. This is consistent with a recent study that found no genomic signature of HR deficiency in 294 breast, ovarian, pancreatic, or prostate cancers with biallelic inactivation of BAP1 [47].

The original study that identified BAP1 as a BRCA1-interacting protein used a yeast two-hybrid assay with cDNA libraries from mouse embryos and human B-cells[23]. Most subsequent screens for BAP1-interacting proteins have used HeLa or Hek293 cells (see Baas, *et al.* [1] and references therein) and none have used DPM cells. Here, using DPM cells in an unbiased proteomic analysis for BAP1-interactors, we report the identification of DNA-PKcs as a major interaction partner of the tumor suppressor BAP1 and the functional characterization of the role of this interaction in NHEJ-mediated DNA repair in DPM cells.

Results

A role for BAP1 in DNA damage repair

To assess the effect of BAP1 on DNA repair at a global cellular level, we first performed knockdown of BAP1 using siRNAs in an DPM cell line, H-Meso, and evaluated genome stability by comet assay. Knockdown of BAP1 resulted in an increase in the length of the comet tail, compared to a negative control, suggesting the involvement of BAP1 in maintenance of genome stability (Figure 1A). To examine the specific domain of BAP1 involved in DNA repair, we performed domain-specific knockdown of BAP1 targeted to known key functional domains by a lentiviral expression system for sgRNA and Cas9 protein (CRISPR/Cas9) using a human mesothelial cell line, MeT-5A. The targeting site of each sgRNA is shown in Figure 1B. Sanger sequence analysis revealed that the site-specific mutations were successfully introduced into cells (Supplementary figure 1). We found that DNA damage induced by radiation (10 Gy), as measured by comet assay, was significantly increased in MeT-5A cells expressing sgRNA targeting ubiquitin C-terminal hydrolase (UCH) domain (sgRNA#1 and #2), near serine 395 (sgRNA#4) and the nuclear localization signal (NLS) domain (sgRNA#5) (Figure 1C). On the other hand, genomic instability was not induced by irradiation in Met-5A cells expressing sgRNA targeting the helical bimodular (HBM) domain (sgRNA#3). We next examined the status of key proteins involved in DSBs repair by western blot analysis. As shown in Figure 1D, the expression of BAP1, DNA-PKcs and γ-H2AX was enhanced in irradiated Met-5A cells transfected with sgRNA targeting specific domains (especially for sgRNA#4), suggesting a role for BAP1 in maintaining genomic stability following radiation damage, possibly dependent on serine 395, and the importance of near serine domain.

Interactional total peptide (ITOP) analysis nominates DNA-PKcs as a major BAP1 interaction partner

To better define the role of BAP1 in DPM cells, in particular to identify its interaction partners in DNA damage-repair pathways, we performed immunoprecipitation (IP) of protein complexes using Flag-tagged wild-type and mutant BAP1 construct (BAP1 C91W) in the human DPM cell line, H-Meso and in HEK293T (293T) cells. This mutant

was chosen because this missense mutation was previously shown to impair ubiquitin hydrolase activity in functional assays [5]. The flow chart of ITOP analysis is shown in Figure 2A. Affinity-purified protein complexes were resolved using SDS-polyacrylamide gel electrophoresis, followed by staining with Coomassie Blue. Separated protein bands were excised and subjected to nano-LC-MS/MS analysis as described in "Materials and Methods". Peptide spectral matches and protein identifications obtained using the Mascot search engine were imported into Scaffold Proteomics software which was used to further validate and cross-tabulate tandem mass spectrometry-based peptide and protein identifications. Peptide counts obtained from co-immunoprecipitated, non-BAP1 fused Flag samples were used for normalization to obtain a fold enrichment score of peptides detected in each Flag-fused BAP1 sample. Protein sequences which co-precipitated with BAP1 (along with their normalized fold enrichment score) were subjected to canonical pathway analysis using the GO Analysis (DICE tool, https://tools.dice-database.org/). This enabled comparisons of each of the protein complexes that showed a strong interaction with BAP1 in both H-Meso and 293T cells. Combining the results of mass spectrometric analysis from H-Meso and 293T cells, GO analysis of the co-IP proteins identified a significant overrepresentation of NHEJ pathway protein, DNA-PKcs (encoded by PRKDC), in association with wild type BAP1 (Figure 2B) but not with BAP1 C91W (results not shown), suggesting that BAP1 may play a role but also in DSB repair via NHEJ. Interestingly, the interactions with BRCA1 and Rad51, which are key proteins for HR, were not detected in this analysis. This finding consistent with previous co-IP studies that have failed to confirm BRCA1 as a significant interaction partner [8, 52]. Nonetheless, recent data confirm that BAP1 can function via both BRCA1-dependent and –independent mechanisms[43]. The complete list of proteins identified in this study is provided in Supplementary table 1.

Next, we investigated the interaction domains of DNA-PKcs and BAP1 by generating deletion mutants of BAP1. The schemas of the deletion mutants are shown in Figure 2C. Co-IP assays revealed that strong interaction between DNA-PKcs and Flag-fused BAP1 was detected in cells expressing deletion mutant#3 and #4, suggesting that the interaction site of DNA-PKcs lies between amino acids 435 to 729 of BAP1, a region that includes the NLS domain (Figure 2D). This interaction site overlaps the previously identified BRCA1 binding site [33]. All other detected kinases that interact with BAP1 wild-type in both H-Meso and 293T cells interacted less strongly than DNA-PKcs (Supplementary table 1). ATM and ATR, two major kinases involved in the response to DSBs, were not observed to interact with BAP1 in our mass spectrometric analysis data. Taken together, among kinases in the NHEJ pathway, DNA-PKcs showed the strongest evidence of interaction with BAP1 even in the absence of DNA damage.

Phosphorylation of BAP1 upon DNA damage

BAP1 is known to be phosphorylated in an ATM-dependent manner at several sites upon DNA damage [12, 22]. Given the key role of phosphorylation events in the DNA damage response and the identification of DNA-PKcs as a putative BAP1 interaction partner, we examined whether double-strand DNA (dsDNA) damage from ionizing radiation (10 Gy) affected the degree of BAP1 phosphorylation. Based on additional LC-MS/MS analyses, we found strong phosphorylation at serine 395 of BAP1 (phosphoBAP1S395) upon ionizing

radiation (Supplementary figure 2 and Supplementary table2). We next sought to examine the role of BAP1 S395 phosphorylation in BAP1-mediated DNA repair. We found that the level of phosphoBAP1S395 in irradiated H-Meso cells expressing BAP1 WT was reduced by pretreatment with the DNA-PKcs inhibitor II, suggesting that DNA repair by DNA-PKcs may be regulated through phosphoBAP1S395 (Figure 3A and Supplementary table 3). In addition, Phos-tag SDS gel analysis showed that overall phosphorylation of BAP1 was increased when dsDNA damage was induced with 0.5μg/ml neocarzinostatin (NCS), but mutation of serine 395 markedly reduced overall BAP1 phosphorylation, indicating that serine 395 is a major phosphorylation site (Figure 3B and Supplementary figure 3). Finally, phosphoBAP1S395 upon DNA damage by NCS was also confirmed using a custom phosphospecific serum to phospho-BAP1-S395 (COVANCE) generated using the peptide sequence CVRPPQQY(pS)DDED (specific detection of this peptide and not the non-phosphorylated peptide was confirmed by ELISA) (Supplementary figure 4). Interestingly, the C91W inactivating mutation in the UCH domain abolished expression of phosphoBAP1S395 (Supplementary table 2). This phenomenon was validated by western blot analysis and immunofluorescent staining. As shown in Figure 3C and 3D, the induction of BAP1 C91W reduced the level of phosphoBAP1S395. These results suggest the possibility that the deubiquitinating activity of BAP1 plays an important role in the process of DNA repair mediated through a phosphoBAP1S395/DNA-PKcs axis.

Phosphorylation changes BAP1 localization

To assess the influence of DNA damage on BAP1 and DNA-PKcs, we next investigated the expression of endogenous BAP1 and DNA-PKcs in MeT-5A and H-Meso cells. Immunofluorescent staining showed nuclear expression of both BAP1 and DNA-PKcs, most apparent in the setting of DNA damage (Figure 4A). Their nuclear localization was disrupted by treatment with 500 nM of DNA-PKcs inhibitor II in the H-Meso cell line (Supplementary figure 5). As shown in Figure 2C, the interaction site for DNA-PKcs maps to the C-terminal of BAP1, and BAP1 has two nuclear localization signal (NLS) sites between amino acids 656–722 at the C terminus, designated NLS1 and NLS2. We then examined the changes of BAP1 localization upon dsDNA damage. NCS (0.5μg/ml)-induced dsDNA damage caused immediate translocation of GFP-fused BAP1 into the nucleus in H-Meso cells. This nuclear translocation occurred within 15 min and GFP-fused BAP1 stayed in the nucleus for more than 3 h (Figure 4B). Interestingly, GFP-BAP1 S395A did not enter the nucleus even upon DNA damage, while GFP-BAP1 C91W did (Figure 4B). Considering that the deubiquitination activity of cells expressing BAP1 S395A is conserved (Figure 4C), phosphoBAP1S395 may influence protein localization only.

Interaction of BAP1 with DNA-PKcs

We next studied interactions between DNA-PKcs and BAP1 including wt and mutant forms with decreased (BAP1 C91W) or increased (BAP1S63C) deubiquitination activity [5], under different conditions in 293T cells (Figure 5A) and the H-Meso DPM cell line (Figure 5B). Cancer cell lines show nearly constitutive expression of DNA-PKcs which does not change markedly upon experimentally induced DNA damage [35]. We noted a similar interaction between wild type BAP1 and DNA-PKcs or Ku70, which are key proteins for NHEJ DNA repair, under irradiated and non-irradiated conditions. 48 hours

after irradiation, this phenomenon was also evident in H-Meso cells expressing BAP1 WT or deubiquitination-proficient BAP1 S63C mutant (Figure 5B). In contrast, while interaction between DNA-PKcs and BAP1 C91W was detected in the absence of irradiation in cells expressing deubiquitination-defective BAP1 C91W mutant, in the setting of DNA damage by irradiation (10 Gy), this interaction was notably decreased, at least partly due to a decrease in the levels of DNA-PKcs protein (Figure 5A and 5B). Hypothesizing that this might be related to increased ubiquitin-mediated degradation of DNA-PKcs, we examined the degree of ubiquitination of DNA-PKcs. This showed that immunoprecipitated DNA-PKcs from irradiated 293T cells that expressed the deubiquitination-defective mutant BAP1 C91W displayed increased K48-linked polyubiquitin (Figure 5C). Intriguingly, overexpression of BAP1 C91W appears to cause an increase in DNA damage in H-Meso cells as measured by γH2AX induction, even in the absence of exogenous DNA damage (Figure 5B, 24 after irradiation). These results suggest that the deubiquitinase activity of BAP1 may be necessary to stabilize protein levels of DNA-PKcs in the setting of DNA damage. Together with our data supporting phosphorylation of BAP1 by DNA-PKcs, these results suggest that BAP1 and DNA-PKcs may target each other to mutually enhance their respective functions, stabilizing the NHEJ DNA repair complex.

Functional effect of BAP1 on the NHEJ pathway

To further investigate a possible role of BAP1 in the NHEJ pathway, nuclear extracts from 293T cells treated with BAP1 siRNA or negative control siRNA were used in a plasmid-based NHEJ assay [21, 31]. Nuclear extracts from 293T cells following BAP1 knockdown showed significantly poorer ligation activity, compared to negative control. Conversely, the introduction of wild-type BAP1 caused increased ligation activity. Rescue experiments using recombinant Flag-fused BAP1 immunoprecipitated from 293T cells showed that NHEJ activity in the plasmid-based NHEJ assay could be restored by wild-type BAP1 but not by the ubiquitin hydrolase-defective BAP1 C91W mutant, implicating the deubiquitination activity of BAP1 in NHEJ (Figure 5D). Together, these results support a major role for BAP1 in NHEJ activity and suggest that DNA repair pathways should be surveyed for synthetic lethal targets in BAP1-deficient cells.

Exploiting the role of BAP1 in NHEJ to enhance DPM therapy

We then examined the effect of BAP1 status on radiation damage enhancement by gemcitabine, reasoning that gemcitabine could help expose a latent DNA repair vulnerability. Previous data have shown that DNA-PK inhibition can enhance radiotherapy response[54]. Three types of shRNA (non-target, BAP1#1, and BAP1#2) were introduced by lentivirus in H-Meso cells and the cells were then treated with gemcitabine with or without irradiation. BAP1 knockdown in H-Meso cells was associated with increased radiation sensitivity (Figure 6A). This result shows that suppressing NHEJ activity by knocking down of BAP1 expression enhanced the sensitivity of H-Meso cells to irradiation, possibly due to combined impairment of NHEJ and HR. A schema outlining a potential therapeutic strategy targeting genomic instability in DPM is shown in Figure 6B.

Discussion

In the present study, we nominate DNA-PKcs as a novel interaction partner of BAP1 in both normal and DPM cells. Our results suggest that dsDNA damage may increase the interaction between BAP1 and DNA-PKcs, and this interaction increases phosphoBAP1S395, resulting in BAP1 translocation into the nucleus in DPM cells. Thus phosphorylation of BAP1 serine 395 appears to be mediated at least in part by DNA-PKcs. BAP1 serine 395 is a known phosphorylation site [6], but its effects and the kinase responsible for this phosphorylation had not previously been identified [7, 37, 42, 52].

In the process of NHEJ DNA repair, nuclear BAP1 is important for maintaining the levels of DNA-PKcs by inhibiting the degradation of DNA-PKcs. We also find that BAP1 mutants with loss of deubiquitination activity or C-terminal deletions impairing nuclear localization and interaction with DNA-PKcs resulted in decreased levels of DNA-PKcs, a key regulator of NHEJ, due to its increased degradation. Considering that mutation in S395 of BAP1 inhibited the nuclear translocation of BAP1 and BAP1 C91W reduced the level of phosphoBAP1S395, the deubiquitination activity of BAP1 not only contributes to the maintenance of DNA-PKcs protein levels, but may also play a role in the regulation of BAP1 localization in DPM. Some studies reported that similarly to BRCA1, BAP1 is required for the effective assembly of key HR factors, such as RAD51 [17, 52]. Ismail and colleagues reported that in human osteosarcoma U2OS cells and human squamous cell carcinoma cells, BAP1 promotes the repair of DSB via HR, and BAP1 has less impact DSB repair via NHEJ in those cells [22]. Yu and colleagues also reported that BAP1 is essential for efficient assembly of the HR factors BRCA1 and RAD51 in chicken DT40 cells, and concluded that BAP1 plays an important role in DSB repair by HR [52]. In contrast to these previous studies, our results suggest the possibility that BAP1 also plays a role in NHEJ-mediated DSB repair, indicating that BAP1 contributes significantly to DNA repair in general in DPM. How this may affect outcomes in DPM is unclear because, unlike other cancer types such as uveal melanoma and renal cell carcinoma, the inactivation of BAP1 does not correlate with poor prognosis in DPM [20, 53]. However, it is notable that, in uveal melanoma, DNA-PKcs (encoded by PRKDC) is more highly expressed in the setting of BAP1 inactivation[10, 26] and this subset is sensitive to DNA-PK inhibition[10]. Further independent evidence is provided by a recent study that identified PRKDC as a synthetic lethal target in BAP1-inactivated of clear cell renal cell carcinoma[30].

Several reports indicate that DPM can be sensitive to high-dose irradiation. For instance, a recent clinical trial involving patients with DPM found improved long-term survival rate using pemetrexed plus cisplatin followed by extrapleural pneumonectomy and radiation, particularly for patients who completed all therapies [25, 34]. Median survival in the overall population was longer than that of patients not receiving irradiation [4, 25]. Several classes of drugs have shown *in vitro* radiation enhancement activity, including taxanes, platinum analogs, topoisomerase inhibitors, and gemcitabine [13]. In particular, gemcitabine has radiation-sensitizing capabilities, as established *in vitro* and in clinical studies [28] based at least in part on specific interference with HR [45]. Consistent with these reports, several studies including our results showed that BAP1 knockdown in BAP1 wild-type cells enhanced the radiation sensitizing effect of gemcitabine, suggesting a possible synergistic

effect due to their induction of impaired NHEJ and HR, respectively [2, 51]. These results suggest that the latent NHEJ deficiency induced by BAP1 inactivation in DPM may be synthetic lethal with inhibition of HR DNA repair mechanisms, indicating a novel therapeutic strategy for targeting the process of DNA repair in DPM. An impairment of NHEJ alone may not lead to carcinogenesis in the absence of extrinsic sources of DNA damage as mutant mice with deletion of Ku70, Ku80, or both show early aging without substantially increased cancer incidence [29]. Consistent with this observation, Kadariya and colleagues reported that the impairment of NHEJ in BAP1-deficient mice may increase their susceptibility to DNA damage from asbestos or other sources [24]. Given our results, NHEJ activity may be constitutively suppressed in BAP1-inactivated DPM through the downregulation of DNA-PKcs (due to unopposed ubiquitination and therefore increased turnover). Use of BAP1 S195 phospho-specific antibody, in conjunction with robust antibodies already available for immunohistochemistry for total BAP1 [40], might allow assessment of BAP1 functional status in DPM and thereby possibly serve as a predictive biomarker for novel therapeutic approaches targeting the latent impairment of DNA repair activity in BAP1-deficient DPM.

In conclusion, we provide the evidence that the direct interaction with BAP1 and DNA-PKcs is associated with phosphorylation by the latter at BAP1 residue S395 in DPM, resulting in maintenance of deubiquitination activity through BAP1 nuclear translocation. The degradation of DNA-PKcs is regulated by deubiquitination by BAP1, which contributes to the process of NHEJ DNA repair. The dependence of efficient NHEJ DNA repair on this BAP1/DNA-PKcs interaction may inform new therapeutic approaches for DPM.

Materials and Methods

Domain specific gene targeting by CRISPR/Cas9

The non-targeted sgRNA sequences and the BAP1 genomic DNA targeting sequences used for the cloning of sgRNAs are shown in Supplementary table 4A. The sgRNA sequence selection and design was performed using online software Optimized CRISPR Design - MIT (http://crispr.mit.edu). pLKO5.sgRNA.EFS.tRFP and pL-CRISPR.SFFV.PAC (Addgene: #57823, #57829) were used as backbone vectors for constitutional sgRNA and Cas9 expression. Lentiviral particles were produced by transient transfection of 293T cells using the calcium-phosphate transfection method. Viral constructs were co-transfected with pMD2.G (Addgene plasmid 12259) and psPAX2 (Addgene plasmid 12260). Lentiviral particles were concentrated using ultracentrifugation.

Peptide and Protein identification by LC-MS/MS

FLAG-tag purified protein complexes were resolved using SDS-polyacrylamide gel electrophoresis followed by brief staining with Coomassie Brilliant Blue and excision of the protein bands. In all samples, prominently stained bands were excised separately to increase the dynamic range encountered during the mass spectrometric analysis of complex protein mixtures and detection of peptides arising from proteins found in less abundant amounts than, for example, BAP1. In situ trypsin digestion of polypeptides in each gel slice was performed and resulting tryptic peptides were purified using a 2-μL

bed volume of Poros 50 R2 (Applied Biosystems, Foster City, CA, USA) reverse-phase beads packed in Eppendorf gel-loading tips [41]. The purified peptides were diluted with 0.1% formic acid and then subjected to nano-liquid chromatography coupled with tandem mass spectrometry (nanoLC-MS/MS) analysis as follows. Peptide mixtures (in 20 μL) were loaded onto a trapping guard column (0.3 × 5 mm Acclaim PepMap 100 C18 cartridge from LC Packings Inc., San Francisco, CA, USA) using an Eksigent nano MDLC system (Eksigent Technologies, Inc. Danaher Corp, Dublin, CA, USA) at a flow rate of 20 μL/min. After washing, the flow was reversed through the guard column and the peptides eluted with a 5–45% acetonitrile gradient over 85 min at a flow rate of 200 nL/min, through a 75-micron x 15-cm fused silica capillary PepMap 100 C18 column (LC Packings). The eluent was directed to a 75-micron (with 10-micron orifice)-fused silica nano-electrospray needle (New Objective, Inc., Woburn, MA, USA). The electrospray ionization voltage was set at 1800. A linear ion quadrupole trap-Orbitrap hybrid analyzer (LTQ-Orbitrap, ThermoFisher) was operated in automatic, data-dependent MS/MS acquisition mode with one full MS scan (450–2,000 m/z) in the Orbitrap analyzer at resolving power of 60, 000 and up to five concurrent MS/MS scans in the LTQ for the five most intense peaks selected from each survey scan. Survey scans were acquired in profile mode and MS/MS scans were acquired in centroid mode. The collision energy was automatically adjusted for the experimental mass (m/z) value of the precursor ions selected for MS/MS. A minimum ion intensity of 2,000 counts was required to trigger an MS/MS spectrum and the dynamic exclusion duration was set at 60 s. Initial protein and peptide identifications from the LC-MS/MS data were performed using the Mascot search engine (Matrix Science, London, UK, version 2.3.02) with the human segment of the Uniprot protein database (20,329 sequences; European Bioinformatics Institute, Swiss Institute of Bioinformatics and Protein Information Resource). The search parameters were as follows: (i) one missed tryptic cleavage site was allowed; (ii) precursor ion mass tolerance,10 ppm; (iii) fragment ion mass tolerance,0.8 Da; and (iv) variable protein modifications were allowed for methionine oxidation, cysteine acrylamide derivatization, and protein N-terminal acetylation. MudPit scoring was typically applied using significance threshold score $p < 0.01$. Decoy database search was always activated and, in general, for merged LS-MS/MS analysis of a gel lane with $p < 0.01$, the false discovery rate averaged around 1%. Scaffold (Proteome Software Inc., Portland, OR, USA, version 4.4.3) was used to further validate and cross-tabulate MS/MS-based peptide and protein identifications. The two search engine results were combined and displayed at 1% FDR. Protein and peptide probability were assigned by the Protein Prophet algorithm [36] was set at 95% with a minimum peptide requirement of 1.

In vitro NHEJ plasmid assay

Cell-free nuclear extracts from 293T cells for NHEJ assay were prepared as described [21, 31]. Briefly, 48 h after transfection, nuclear extracts from 2×10^7 cells were purified with an NE-PER protein extraction kit (Thermo). The nuclear pellet was then resuspended in two volumes of nuclear extraction buffer (20 mM Tris–HCl pH 7.6, 1 mM DTT, 2 mM EDTA, 20% glycerol, 500 mM NaCl, and protease inhibitors) and incubated for 30 min on ice. Nuclear extracts were then clarified for 30 min at 40,000g and dialyzed overnight against dialysis buffer D (20 mM Tris–HCl pH 7.6, 1 mM EDTA, 1 mM DTT, 20% glycerol, 25 mM NaCl, and 0.2 mM PMSF). The end-joining reaction was performed in a final volume

of 30μl by incubation of 50ng of *Sal I*-digested pBS-SK(−) plasmid with 1μg or 5μg of nuclear extract for 1h at 37°C in buffer E (50 mM Tris–HCl pH 7.6, 5 mM $MgCl_2$, 1 mM ATP, 1 mM DTT, 50 μM dNTP, 80 mM NaCl, and protease inhibitors). The reaction was stopped by RNAse treatment (0.25 μg/μl of RNAse for 10 min at 37°C) followed by proteinase K treatment (0.5% SDS, 50 mM EDTA, and 1 μg/μl of proteinase K at 37°C for 1h). DNA was purified by phenol and chloroform extraction and recovered by ethanol precipitation. Linear plasmids and multiple ligated linear plasmids were quantified by *Sal I*-cleaved site-specific (604–740 bp) and non-cleaved site (1,500–1,650 bp) TaqMan probes (Invitrogen) (Supplementary table 4B), using an iCycler Real-Time PCR Detection System.

Ubiquitin-AMC assay

All procedures were performed as described previously [5]. Wild-type and mutant Bap1-flag proteins were immunopurified with anti-Flag beads (30 μl) and eluted with four washes (50 μl/each) of NP-40 buffer containing 2 mM DTT, 5% glycerol, and 0.5 mg of three-Flag peptide/ml. To assess the UCH activity, the fluorogenic substrate 7-amido-4-methylcoumarin-derivatized ubiquitin (ubiquitin-AMC; Boston Biochem) was diluted to a final concentration of 340 nM in 190 μl of the assay buffer (50 mM HEPES [pH 7.5], 0.5 mM EDTA, and 1 mM DTT). Samples were incubated for 2 h at room temperature and levels of hydrolyzed AMC were measured by excitation at 380 nm and emission at 460 nm. UCH-L3 (400 μg; Boston Biochem) was used as a positive control and 10 μl of BAP1-Flag elution was used in each assay. All samples were tested in triplicate.

Supplementary Material

Refer to Web version on PubMed Central for supplementary material.

Acknowledgements

We are grateful to Ronald C. Hendrickson (Proteomics & Microchemistry, Memorial Sloan Kettering Cancer Center), Sho Fujisawa (Molecular Cytology, Memorial Sloan Kettering Cancer Center) and Toshiki Terao, Rina Nishiyama and Reiko Kondo (Okayama University, Medical School) for providing technical assistance and opportunities to discuss this work.

Financial Support:

DOD CMDRP grant W81XWH 15 1 0210 (Zauderer)

Data availability

Not applicable

References

Uncategorized References

1. Baas R, JvdW F, Bleijerveld OB, van Attikum H, Sixma TK. Proteomic analysis identifies novel binding partners of BAP1. PLoS One 2021; 16: e0257688. [PubMed: 34591877]
2. Blackford AN, Jackson SP. ATM, ATR, and DNA-PK: The Trinity at the Heart of the DNA Damage Response. Molecular Cell 2017; 66: 801–817. [PubMed: 28622525]

3. Blunt T, Finnie NJ, Taccioli GE, Smith GC, Demengeot J, Gottlieb TM et al. Defective DNA-dependent protein kinase activity is linked to V(D)J recombination and DNA repair defects associated with the murine scid mutation. Cell 1995; 80: 813–823. [PubMed: 7889575]
4. Boons CC, VANT MW, Burgers JA, Beckeringh JJ, Wagner C, Hugtenburg JG. The value of pemetrexed for the treatment of malignant pleural mesothelioma: a comprehensive review. Anticancer Research 2013; 33: 3553–3561. [PubMed: 24023280]
5. Bott M, Brevet M, Taylor BS, Shimizu S, Ito T, Wang L et al. The nuclear deubiquitinase BAP1 is commonly inactivated by somatic mutations and 3p21.1 losses in malignant pleural mesothelioma. Nature Genetics 2011; 43: 668–672. [PubMed: 21642991]
6. Bueno R, Stawiski EW, Goldstein LD, Durinck S, De Rienzo A, Modrusan Z et al. Comprehensive genomic analysis of malignant pleural mesothelioma identifies recurrent mutations, gene fusions and splicing alterations. Nature Genetics 2016; 48: 407–416. [PubMed: 26928227]
7. Cantin GT, Yi W, Lu B, Park SK, Xu T, Lee JD et al. Combining protein-based IMAC, peptide-based IMAC, and MudPIT for efficient phosphoproteomic analysis. Journal of proteome research 2008; 7: 1346–1351. [PubMed: 18220336]
8. Cary RB, Peterson SR, Wang J, Bear DG, Bradbury EM, Chen DJ. DNA looping by Ku and the DNA-dependent protein kinase. Proceedings of the National Academy of Sciences of the United States of America 1997; 94: 4267–4272. [PubMed: 9113978]
9. Chau C, van Doorn R, van Poppelen NM, van der Stoep N, Mensenkamp AR, Sijmons RH et al. Families with BAP1-Tumor Predisposition Syndrome in The Netherlands: Path to Identification and a Proposal for Genetic Screening Guidelines. Cancers 2019; 11. [PubMed: 31861498]
10. Dogrusoz M, Ruschel Trasel A, Cao J, Çolak S, van Pelt SI, Kroes WGM et al. Differential Expression of DNA Repair Genes in Prognostically-Favorable versus Unfavorable Uveal Melanoma. Cancers 2019; 11. [PubMed: 31861498]
11. Douglas P, Sapkota GP, Morrice N, Yu Y, Goodarzi AA, Merkle D et al. Identification of in vitro and in vivo phosphorylation sites in the catalytic subunit of the DNA-dependent protein kinase. The Biochemical journal 2002; 368: 243–251. [PubMed: 12186630]
12. Eletr ZM, Yin L, Wilkinson KD. BAP1 is phosphorylated at serine 592 in S-phase following DNA damage. FEBS Letters 2013; 587: 3906–3911. [PubMed: 24211834]
13. Ewald B, Sampath D, Plunkett W. H2AX phosphorylation marks gemcitabine-induced stalled replication forks and their collapse upon S-phase checkpoint abrogation. Molecular Cancer Therapeutics 2007; 6: 1239–1248. [PubMed: 17406032]
14. Febres-Aldana CA, Fanaroff R, Offin M, Zauderer MG, Sauter JL, Yang SR, et al. Diffuse Pleural Mesothelioma: Advances in Molecular Pathogenesis, Diagnosis and Treatment. Ann Rev of Pathol: Mechanisms of Disease 2023 Sep 18. doi: 10.1146/annurev-pathol-042420-092719. Online ahead of print.
15. Fennell DA, King A, Mohammed S, Branson A, Brookes C, Darlison L et al. Rucaparib in patients with BAP1-deficient or BRCA1-deficient mesothelioma (MiST1): an open-label, single-arm, phase 2a clinical trial. Lancet Respir Med 2021; 9: 593–600. [PubMed: 33515503]
16. Ghafoor A, Mian I, Wagner C, Mallory Y, Agra MG, Morrow B et al. Phase 2 Study of Olaparib in Malignant Mesothelioma and Correlation of Efficacy With Germline or Somatic Mutations in BAP1 Gene. JTO Clin Res Rep 2021; 2: 100231. [PubMed: 34661178]
17. Guo G, Chmielecki J, Goparaju C, Heguy A, Dolgalev I, Carbone M et al. Whole-exome sequencing reveals frequent genetic alterations in BAP1, NF2, CDKN2A, and CUL1 in malignant pleural mesothelioma. Cancer research 2015; 75: 264–269. [PubMed: 25488749]
18. Harbour JW, Onken MD, Roberson ED, Duan S, Cao L, Worley LA et al. Frequent mutation of BAP1 in metastasizing uveal melanomas. Science 2010; 330: 1410–1413. [PubMed: 21051595]
19. Hartlerode AJ, Scully R. Mechanisms of double-strand break repair in somatic mammalian cells. The Biochemical journal 2009; 423: 157–168. [PubMed: 19772495]
20. Hmeljak J, Sanchez-Vega F, Hoadley KA, Shih J, Stewart C, Heiman D et al. Integrative Molecular Characterization of Malignant Pleural Mesothelioma. Cancer Discovery 2018; 812:1548–1565.
21. Iliakis G, Rosidi B, Wang M, Wang H. Plasmid-based assays for DNA end-joining in vitro. Methods in molecular biology (Clifton, NJ) 2006; 314: 123–131.

22. Ismail IH, Davidson R, Gagne JP, Xu ZZ, Poirier GG, Hendzel MJ. Germline mutations in BAP1 impair its function in DNA double-strand break repair. Cancer Research 2014; 74: 4282–4294. [PubMed: 24894717]
23. Jensen DE, Proctor M, Marquis ST, Gardner HP, Ha SI, Chodosh LA et al. BAP1: a novel ubiquitin hydrolase which binds to the BRCA1 RING finger and enhances BRCA1-mediated cell growth suppression. Oncogene 1998; 16: 1097–1112. [PubMed: 9528852]
24. Kadariya Y, Cheung M, Xu J, Pei J, Sementino E, Menges CW et al. Bap1 Is a Bona Fide Tumor Suppressor: Genetic Evidence from Mouse Models Carrying Heterozygous Germline Bap1 Mutations. Cancer Research 2016; 76: 2836–2844. [PubMed: 26896281]
25. Krug LM, Pass HI, Rusch VW, Kindler HL, Sugarbaker DJ, Rosenzweig KE et al. Multicenter phase II trial of neoadjuvant pemetrexed plus cisplatin followed by extrapleural pneumonectomy and radiation for malignant pleural mesothelioma. Journal of Clinical Oncology 2009; 27: 3007–3013. [PubMed: 19364962]
26. Kuznetsoff JN, Owens DA, Lopez A, Rodriguez DA, Chee NT, Kurtenbach S et al. Dual Screen for Efficacy and Toxicity Identifies HDAC Inhibitor with Distinctive Activity Spectrum for BAP1-Mutant Uveal Melanoma. Mol Cancer Res 2021; 19: 215–222. [PubMed: 33077485]
27. Kwon J, Lee D, Lee SA. BAP1 as a guardian of genome stability: implications in human cancer. Exp Mol Med 2023; 55: 745–754. [PubMed: 37009801]
28. Lawrence TS, Eisbruch A, McGinn CJ, Fields MT, Shewach DS. Radiosensitization by gemcitabine. Oncology (Williston Park, NY) 1999; 13: 55–60.
29. Li H, Vogel H, Holcomb VB, Gu Y, Hasty P. Deletion of Ku70, Ku80, or both causes early aging without substantially increased cancer. Molecular and cellular biology 2007; 27: 8205–8214. [PubMed: 17875923]
30. Liu Z, Lin D, Zhou Y, Zhang L, Yang C, Guo B et al. Exploring synthetic lethal network for the precision treatment of clear cell renal cell carcinoma. Sci Rep 2022; 12: 13222. [PubMed: 35918352]
31. Ma Y, Lieber MR. In vitro nonhomologous DNA end joining system. Methods in enzymology 2006; 408: 502–510. [PubMed: 16793389]
32. Mahaney BL, Meek K, Lees-Miller SP. Repair of ionizing radiation-induced DNA double-strand breaks by non-homologous end-joining. The Biochemical journal 2009; 417: 639–650. [PubMed: 19133841]
33. Masoomian B, Shields JA, Shields CL. Overview of BAP1 cancer predisposition syndrome and the relationship to uveal melanoma. Journal of current ophthalmology 2018; 30: 102–109. [PubMed: 29988936]
34. Minatel E, Trovo M, Polesel J, Baresic T, Bearz A, Franchin G et al. Radical pleurectomy/decortication followed by high dose of radiation therapy for malignant pleural mesothelioma. Final results with long-term follow-up. Lung cancer 2014; 83: 78–82. [PubMed: 24216141]
35. Moll U, Lau R, Sypes MA, Gupta MM, Anderson CW. DNA-PK, the DNA-activated protein kinase, is differentially expressed in normal and malignant human tissues. Oncogene 1999; 18: 3114–3126. [PubMed: 10340383]
36. Nesvizhskii AI, Keller A, Kolker E, Aebersold R. A statistical model for identifying proteins by tandem mass spectrometry. Analytical Chemistry 2003; 75: 4646–4658. [PubMed: 14632076]
37. Olsen JV, Blagoev B, Gnad F, Macek B, Kumar C, Mortensen P et al. Global, in vivo, and site-specific phosphorylation dynamics in signaling networks. Cell 2006; 127: 635–648. [PubMed: 17081983]
38. Passiglia F, Righi L, Bironzo P, Listì A, Farinea G, Capelletto E et al. Niraparib plus Dostarlimab in Pleural Mesothelioma or Non-Small Cell Lung Cancer harboring HRR mutations: interim results of the UNITO-001 phase 2 prospective trial. Clin Cancer Res 2023.
39. Rathkey D, Khanal M, Murai J, Zhang J, Sengupta M, Jiang Q et al. Sensitivity of Mesothelioma Cells to PARP Inhibitors Is Not Dependent on BAP1 but Is Enhanced by Temozolomide in Cells With High-Schlafen 11 and Low-O6-methylguanine-DNA Methyltransferase Expression. Journal of Thoracic Oncology 2020; 15: 843–859. [PubMed: 32004714]
40. Righi L, Duregon E, Vatrano S, Izzo S, Giorcelli J, Rondon-Lagos M et al. BRCA1-Associated Protein 1 (BAP1) Immunohistochemical Expression as a Diagnostic Tool in Malignant Pleural

Mesothelioma Classification: A Large Retrospective Study. Journal of Thoracic Oncology 2016; 11: 2006–2017. [PubMed: 27422796]

41. Sebastiaan Winkler G, Lacomis L, Philip J, Erdjument-Bromage H, Svejstrup JQ, Tempst P. Isolation and mass spectrometry of transcription factor complexes. Methods 2002; 26: 260–269. [PubMed: 12054882]
42. Serakinci N, Christensen R, Graakjaer J, Cairney CJ, Keith WN, Alsner J et al. Ectopically hTERT expressing adult human mesenchymal stem cells are less radiosensitive than their telomerase negative counterpart. Experimental Cell Research 2007; 313: 1056–1067. [PubMed: 17274981]
43. Singh A, Busacca S, Gaba A, Sheaff M, Poile C, Nakas A et al. BAP1 loss induces mitotic defects in mesothelioma cells through BRCA1-dependent and independent mechanisms. Oncogene 2023; 42: 572–585. [PubMed: 36550359]
44. Testa JR, Cheung M, Pei J, Below JE, Tan Y, Sementino E et al. Germline BAP1 mutations predispose to malignant mesothelioma. Nature Genetics 2011; 43: 1022–1025. [PubMed: 21874000]
45. Wachters FM, van Putten JW, Maring JG, Zdzienicka MZ, Groen HJ, Kampinga HH. Selective targeting of homologous DNA recombination repair by gemcitabine. International journal of radiation oncology, biology, physics 2003; 57: 553–562. [PubMed: 12957269]
46. Walker JR, Corpina RA, Goldberg J. Structure of the Ku heterodimer bound to DNA and its implications for double-strand break repair. Nature 2001; 412: 607–614. [PubMed: 11493912]
47. Westphalen CB, Fine AD, Andre F, Ganesan S, Heinemann V, Rouleau E et al. Pan-cancer Analysis of Homologous Recombination Repair-associated Gene Alterations and Genome-wide Loss-of-Heterozygosity Score. Clin Cancer Res 2022; 28: 1412–1421. [PubMed: 34740923]
48. Wiesner T, Obenauf AC, Murali R, Fried I, Griewank KG, Ulz P et al. Germline mutations in BAP1 predispose to melanocytic tumors. Nature Genetics 2011; 43: 1018–1021. [PubMed: 21874003]
49. Yaneva M, Kowalewski T, Lieber MR. Interaction of DNA-dependent protein kinase with DNA and with Ku: biochemical and atomic-force microscopy studies. The EMBO journal 1997; 16: 5098–5112. [PubMed: 9305651]
50. Yang H, Xu D, Gao Y, Schmid RA, Peng RW. The Association of BAP1 Loss-of-Function With the Defect in Homologous Recombination Repair and Sensitivity to PARP-Targeted Therapy. Journal of Thoracic Oncology 2020; 15: e88–e90. [PubMed: 32471567]
51. Yap TA, Aerts JG, Popat S, Fennell DA. Novel insights into mesothelioma biology and implications for therapy. Nature Reviews Cancer 2017; 17: 475–488. [PubMed: 28740119]
52. Yu H, Pak H, Hammond-Martel I, Ghram M, Rodrigue A, Daou S et al. Tumor suppressor and deubiquitinase BAP1 promotes DNA double-strand break repair. Proceedings of the National Academy of Sciences of the United States of America 2014; 111: 285–290. [PubMed: 24347639]
53. Zauderer MG, Bott M, McMillan R, Sima CS, Rusch V, Krug LM et al. Clinical characteristics of patients with malignant pleural mesothelioma harboring somatic BAP1 mutations. Journal of Thoracic Oncology 2013; 8: 1430–1433. [PubMed: 24128712]
54. Zenke FT, Zimmermann A, Sirrenberg C, Dahmen H, Kirkin V, Pehl U et al. Pharmacologic Inhibitor of DNA-PK, M3814, Potentiates Radiotherapy and Regresses Human Tumors in Mouse Models. Molecular Cancer Therapeutics 2020; 19: 1091–1101. [PubMed: 32220971]

A

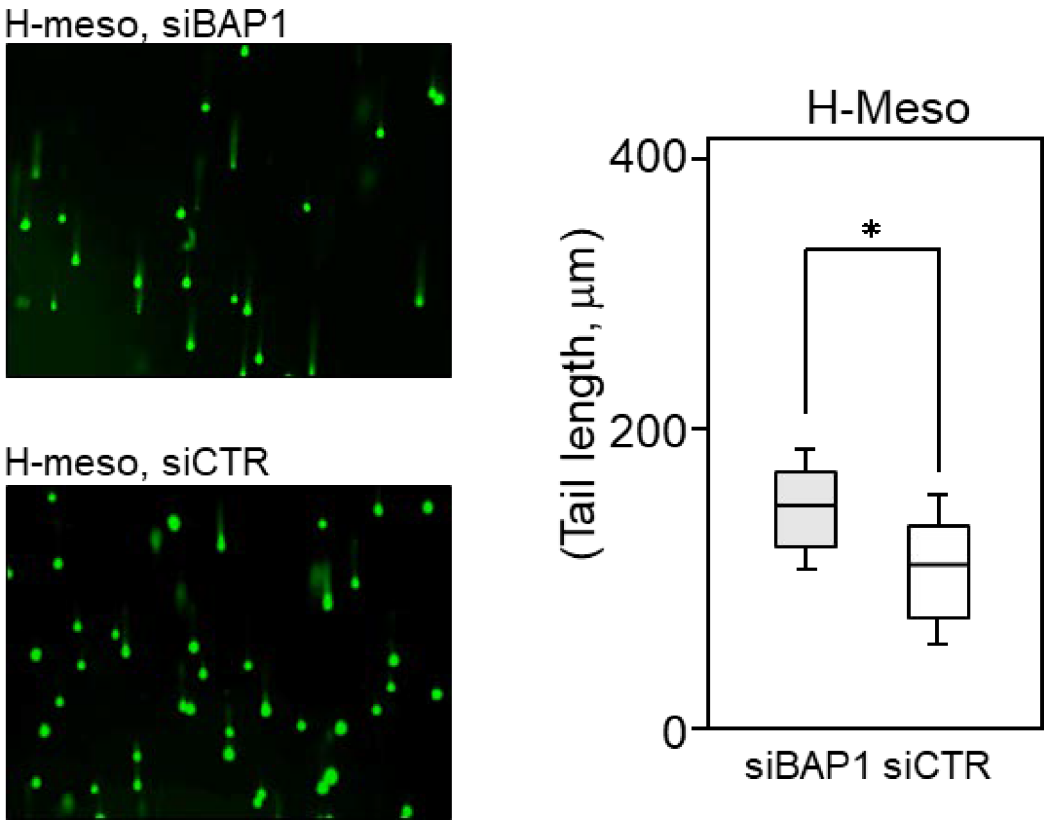

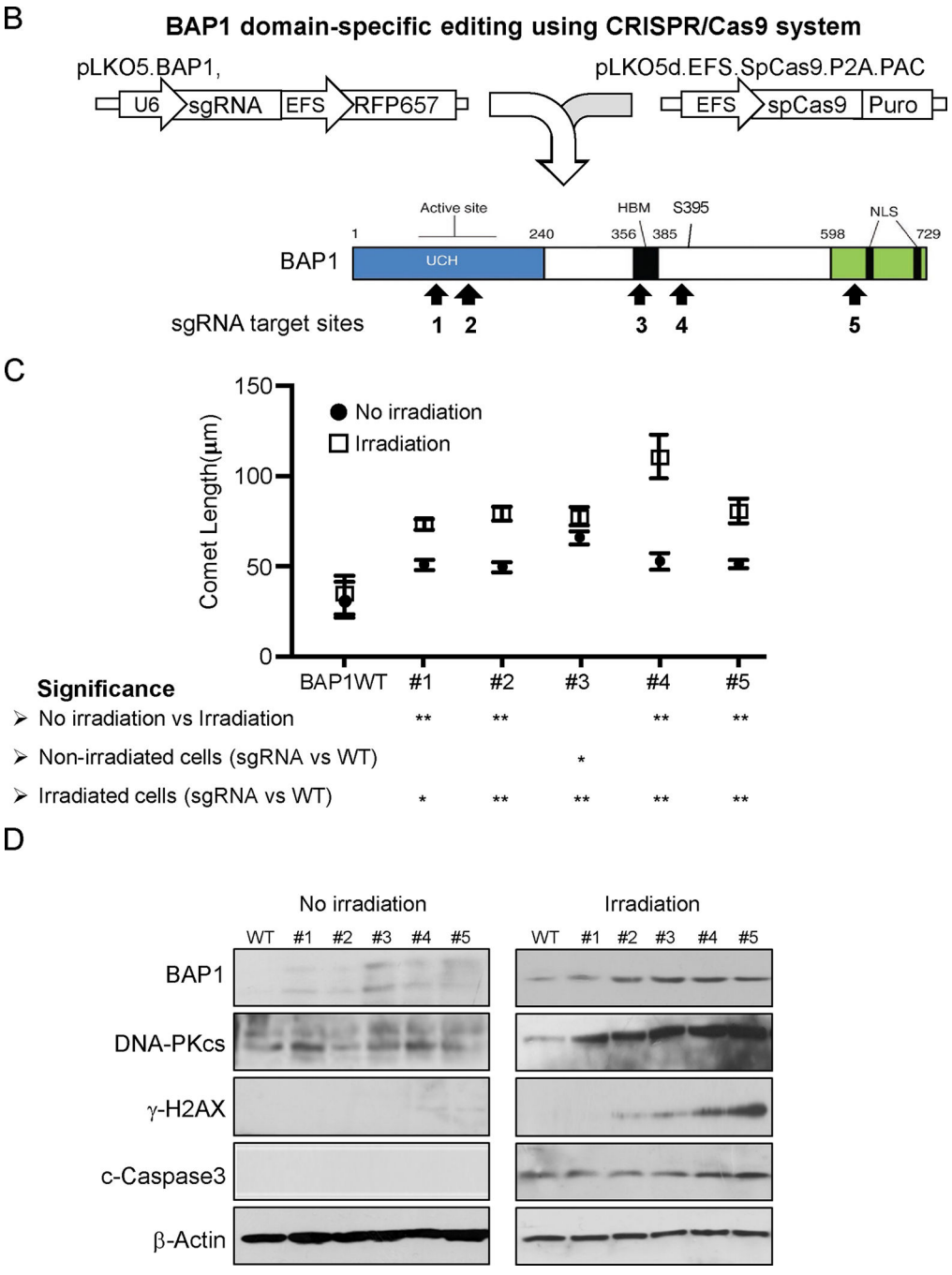

Figure 1: Comet assay analysis for genomic instability caused by genomic alteration of BAP1.

(A) H-Meso cells were transfected with siBAP1 and negative-control siRNA (siCTR). DNA damage were detected by COMET assay, 48h after transfection of siRNA. Representative images were shown. The plot shows the mean tail length of 50 comets +/− SD. Tails of 300–500 μm length, related to the number of DSBs, were counted for each sample (*$p < 0.05$). (B) The location of sgRNAs targeting the ubiquitin C-terminal hydrolase (UCH) domain (sgRNA#1, #2 and #3), the helical bimodular (HBM) domain (sgRNA#4 and #5), near serine 395 site (sgRNA#6) and the nuclear localization signal (NLS) domain (sgRNA#7) are shown

on the schematic diagram of human BAP1. (C) Visualization of DSBs by the comet assay in MeT-5A cells. MeT-5A cells were transected with each sgRNA.EFS.tRFP expression lentiviral vectors followed by the transfection of spCas9-Puro expression lentiviral vectors. The dots or squares shows mean tail length of 50 to 400 comets ± SE. *P < 0.05 and ** P < 0.01. (D) Protein expression of BAP1, DNA-PKCs, Rad5, γH2AX, cleaved Caspase3 and beta-Actin in Met5A cells with or without irradiation. The lane numbers correspond to the number of the sgRNAs targeting the BAP1 domains.

A

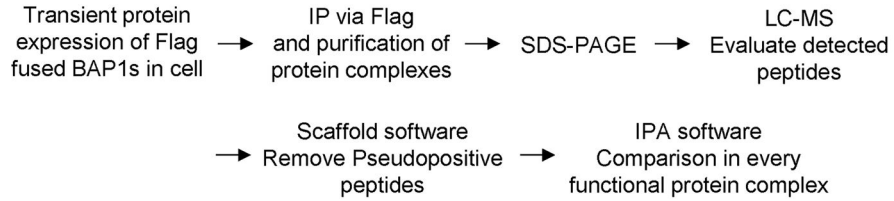

B

GO_term_id	GO_term_def	P	P_FDR_adjusted	Genes
GO:0006281	DNA repair	1.78E-05	4.16E-04	HIST1H4I, MCM3, MCM5, MCM7, MRE11A, MTA1, NONO, NPM1, PDS5A, PDS5B, **PRKDC**, PRPF19, RAD50, RPS3, RUVBL1, RUVBL2, SFPQ, SMC1A, SMC3, SMCHD1, SSRP1, TNKS1BP1, TRIM28, UBA52, VCP, XRCC5
GO:0006302	double-strand break repair	2.21E-05	5.04E-04	HIST1H4I, MCM3, MCM5, MCM7, MRE11A, MTA1, **PRKDC**, PRPF19, RAD50, SFPQ, SMCHD1, TNKS1BP1, VCP, XRCC5
GO:0006303	double-strand break repair via nonhomologous end joining	1.19E-03	1.57E-02	HIST1H4I, MRE11A, **PRKDC**, PRPF19, RAD50, XRCC5
GO:0000727	double-strand break repair via break-induced replication	1.30E-03	1.60E-02	MCM3, MCM5, MCM7

C

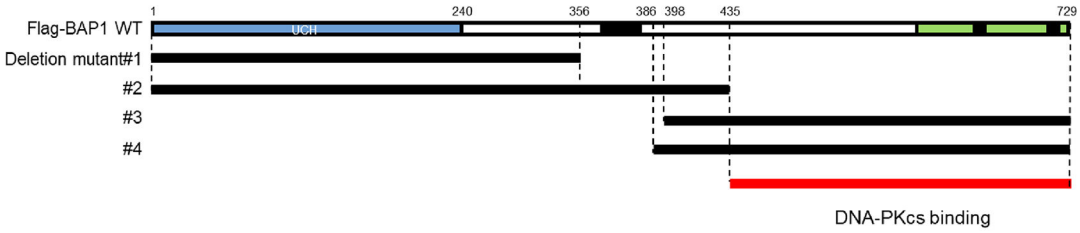

D

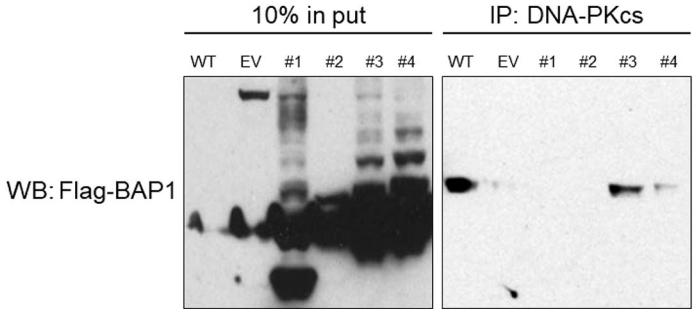

Figure 2: Analysis of BAP1 interacting proteins by Interactional Total Peptide (ITOP) analysis.

(A) Procedure of ITOP analysis. (B) The top gene sets related to DNA repair upregulated in BAP1-WT transfected 293T and H-Meso cells, compared to parental cells are displayed. Listed genes are from peptide sequences detected by LC/MS of immunoprecipitated samples. (C) The schemas of deletion mutants of BAP1. Putative DNA-PKcs binding site is shown as red bar. (D) 293T cells were transfected with the indicated expression plasmids or parental 3xFlag vector. Co-IP assay was performed using anti-DNA-PKcs antibody and Flag antibody. 10% of total cell extract was preserved for input. SDS-Page was used to denature

the proteins and separate them with respect to the size of immunopurified samples. Each protein was detected by Western blot assay.

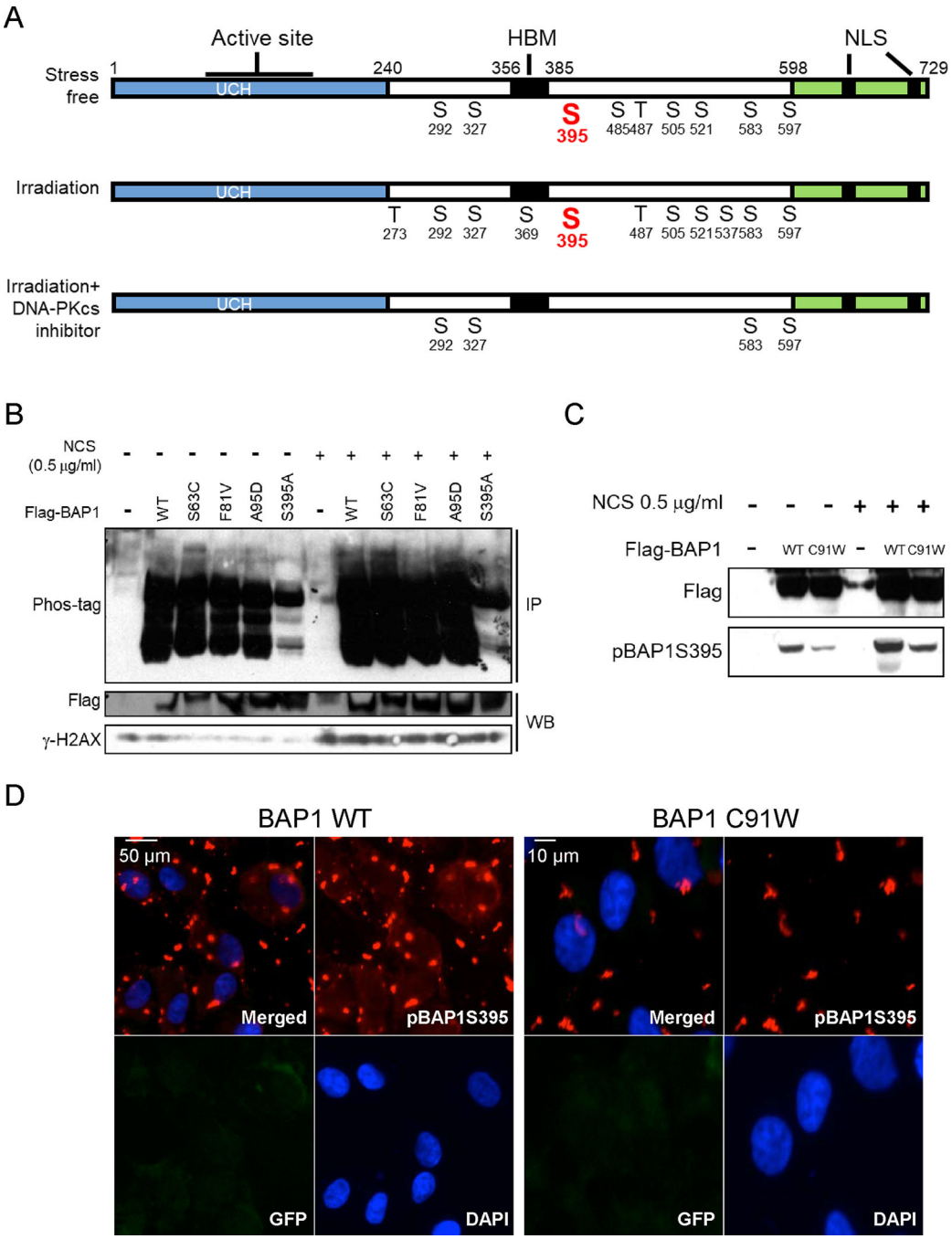

Figure 3: Analysis of phosphorylation sites on BAP1.

(A) Each phosphorylation site detected by LC-MS is shown by the amino acid symbols. The presence of phosphorylation sites was observed between threonine 273 and serine 597. Two kinds of protease were used to perform a more detailed mapping of phosphorylation sites, especially in the UCH domain, but no phosphorylation was detected in the first 240 amino acid residues. (B) Phosphorylation of Flag-tagged BAP1 was detected in H-Meso cells by WB analysis using Phos-Tag SDS gel. (C) Detection of phosphoBAP1S395. One hour after the treatment with NCS or control, cell lysates from H-Meso cells that expressed

Flag-BAP1wt, Flag-BAP1C91W, and Flag as negative control were subjected to western blot analysis. (D) Immunofluorescent staining study of phosphoBAP1S395. H-Meso cells expressing GFP-fused BAP1 WT or BAP1 C91W were used in this study. Red: Green: Blue = phosphoBAP1S395: H2AX: DAPI

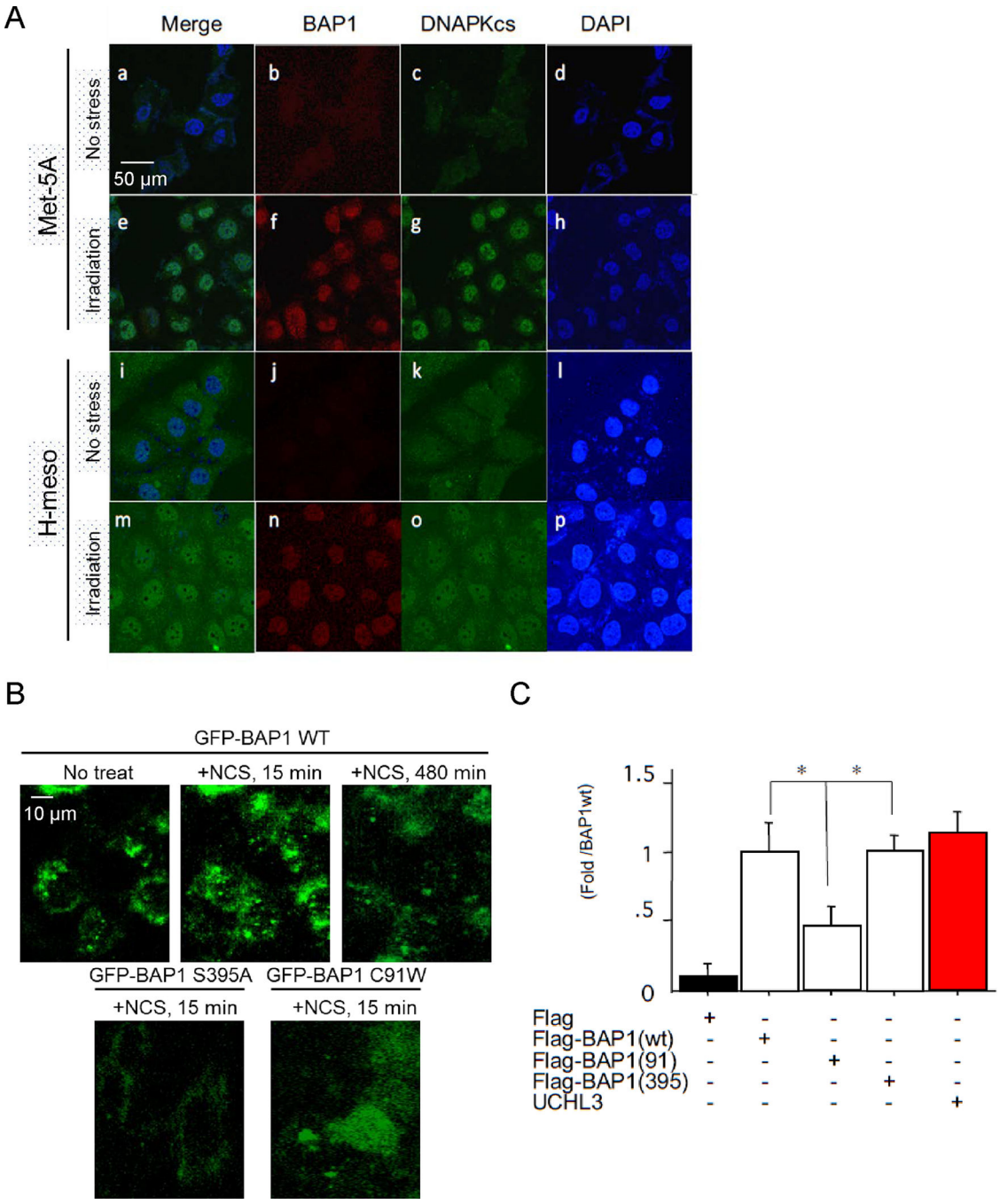

Figure 4: BAP1 protein expression in the (a-h) mesothelium cell MeT-5A and (i- p) DPM cell line H-Meso.

(A) The localization of BAP1 in the DPM cell line H-Meso was examined by immunofluorescence. (Red: Green: Blue = BAP1: DNA-PKcs: DAPI) (a, b, c, d, i, j, k, l) normal conditions, (e, f, g, h, m, n, o, p) 1hr after X ray Irradiation (10Gy). (B) The time-course of BAP1 localization in the DPM cell line H-Meso was examined by immunofluorescence. (C) Ub AMC assay. Flag-fused BAP1 plasmid and parental 3xFlag vector were transfected into H-Meso cells. (*$p < 0.05$).

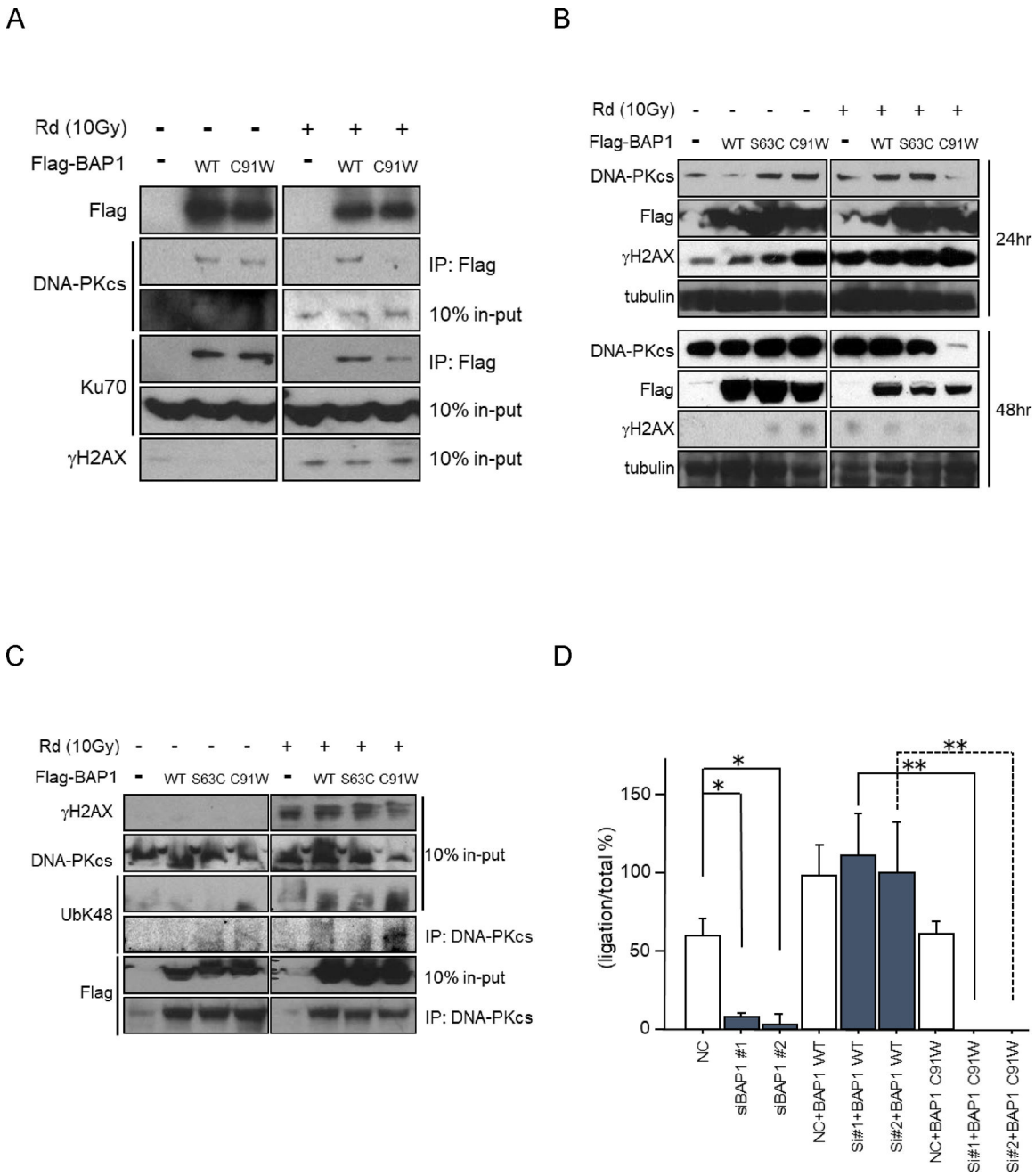

Figure 5: Relationship between BAP1 and DNA-PK.

(A) Flag-fused BAP1-WT and mutated BAP1 were transfected into 293T cells. IP was performed 24 h after DNA damage by X-ray. (B) Western blot analysis of H-Meso cells. Whole cell lysate was collected 24 and 48 h after DNA damage by X-ray. Five micrograms of total protein were loaded into each well. (C) Flag-fused BAP1-wt and mutated BAP1 were transfected into 293T cells. IP was performed 24 h after DNA damage by X-ray. (D) Plasmid-based NHEJ assays were performed using 293T cells (*P < 0.05, **P < 0.01). NC: negative control.

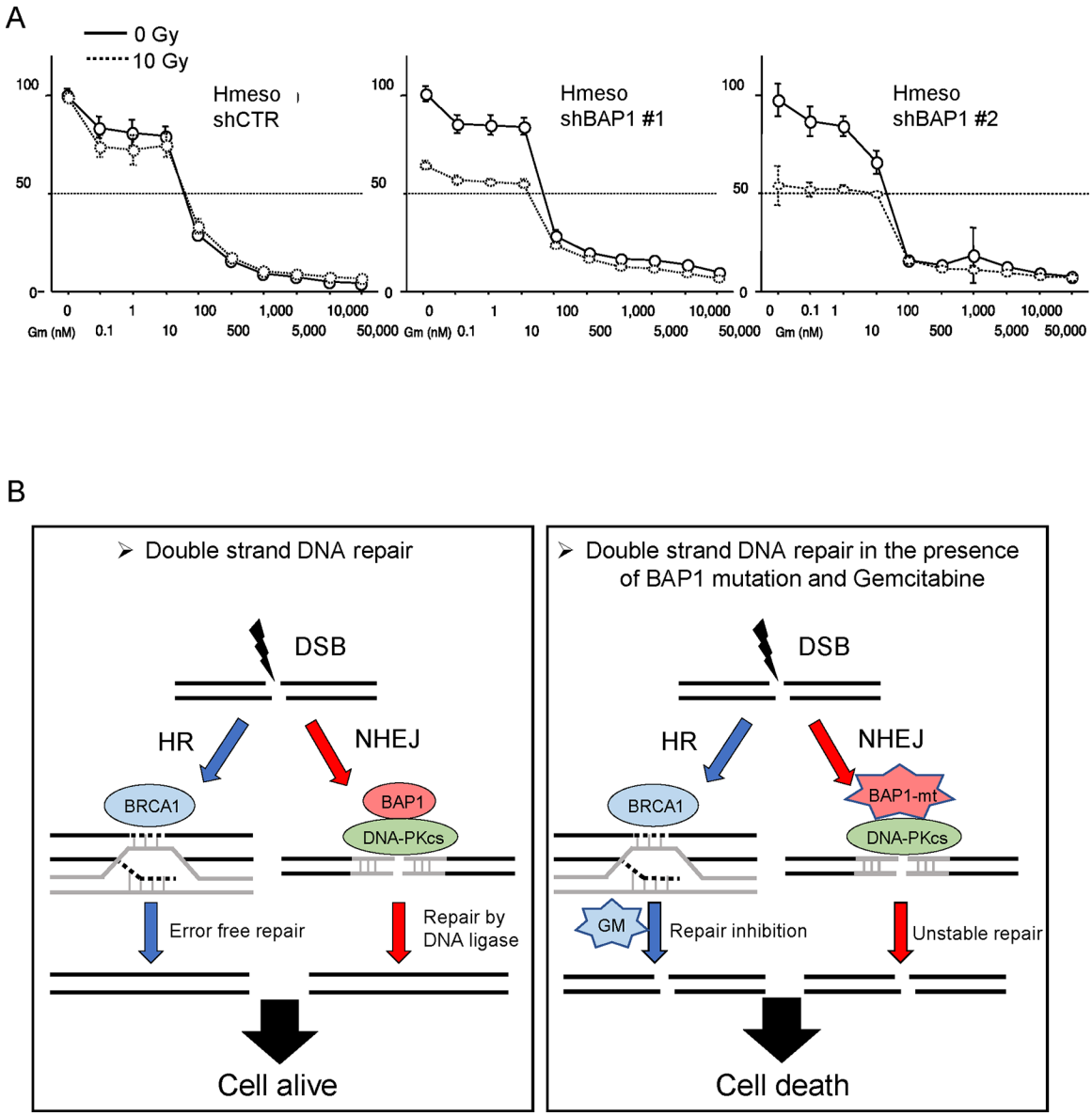

Figure 6: Therapeutic potential of targeting latent genomic instability induced by BAP1 loss in DPM.

(A) Effect of BAP1 shRNA knockdown on the growth of H-Meso cells was examined in cells treated with Gemcitabine with or without X-irradiation (10 Gy) for 96 h prior to determination of cell viability. Alamar blue assay was performed to estimate cell viability. (B) Model for targeting genomic instability in DPM (Lt, normal cell, Rt, abnormal cell with BAP1 mutation). DSB: Double strand break, HR: homologous recombination, NHEJ: non-homologous end joining, GM: Gemcitabine